RSC Sustainability

ROYAL SOCIETY OF CHEMISTRY

PAPER

View Article Online
View Journal | View Issue

Cite this: *RSC Sustainability*, 2025, **3**, 1774

Co-pyrolysis of low-value wood sawdust and non-recyclable plastics into char: effect of plastic loading on char yield and its properties

Ranjeet Kumar Mishra

Co-pyrolysis of biomass and plastics is essential to improve the quality and yield of pyrolytic products, optimise energy recovery, and mitigate plastic waste, providing a sustainable approach to waste valorisation. This study examined char production from the co-pyrolysis of biomass and plastic in a semi-batch reactor at 500 °C with a heating rate of 10 °C min^{-1} and a nitrogen gas flow rate of 100 mL min^{-1}. JCT and NRPET were physically mixed at 30, 50%, and 80% wt%, respectively. The physicochemical properties of biomass and plastics confirmed their suitability as pyrolysis feedstocks. TGA-FTIR results confirmed that the addition of NRPET at 30, 50 and 80 wt% with JCT significantly increased the hydrocarbons and reduced the formation of CO_2, CO and oxygenated compounds. Results showed that blending of non-recyclable PET (NRPET) with Jungle Cork Tree (JCT) at 30%, 50%, and 80% reduced char yield by 5.27%, 9.07%, and 12.47%, respectively. Additionally, the blending of JCT and NRPET improved the properties of the char, such as carbon content (22.59%), heating value (6.17 MJ kg^{-1}), bulk density (200.11 kg m^{-3}), and electrical conductivity. The blending process also led to a significant reduction in the oxygen content (18.05%) and surface area (30.78 m^2 g^{-1}) of the char. FTIR analysis showed a loss of undesirable functional groups, while Raman spectroscopy revealed an increased I_D/I_G ratio. Finally, SEM analysis indicated that the incorporation of plastics increased the hardness and reduced the roughness of the char, enhancing its suitability for energy storage or carbon-based material applications.

Received 25th November 2024
Accepted 17th February 2025

DOI: 10.1039/d4su00739e

rsc.li/rscsus

Sustainability spotlight

"Co-pyrolysis of low-value wood sawdust and non-recyclable plastics into char: effect of plastic loading on char yield and its properties" aligns with the United Nations Sustainable Development Goals (SDGs), particularly SDG 12 (Responsible Consumption and Production) and SDG 13 (Climate Action). By integrating low-value biomass and non-recyclable plastics into a co-pyrolysis process, the study addresses pressing global issues of waste management and resource recovery. It explores the effect of plastic loading on char yield and properties, providing insights into optimizing co-pyrolysis for creating high-value char with enhanced physicochemical attributes. The valorization of these waste streams into functional carbon-based products not only reduces environmental pollution but also supports the circular economy by converting waste into resources. This research contributes to sustainable innovation in waste-to-energy technologies, offering scalable solutions to reduce landfill dependency, lower greenhouse gas emissions, and enhance material efficiency, thereby supporting climate resilience and sustainable resource management.

1 Introduction

Plastics have become indispensable worldwide due to their convenience, adaptability, and low-cost.[1] Modern society relies heavily on plastics, making their removal from daily life nearly unfeasible. The rapid pace of global modernization, coupled with population growth, has significantly increased the demand for energy, food, technology, and consumer products. Consequently, waste generation has surged, with food and green waste accounting for 44% and plastic waste comprising 12% of the total.[2] Since 1950, annual plastic production has grown from 2 million tonnes (MT) to 381 MT by 2018, generating 464 MT of plastic waste each year.[3] Globally, approximately 20% of plastic waste is recycled, 25% is incinerated, and the remaining 55% is disposed of in landfills or dumpsites.[4] Plastics degrade exceptionally slowly in the environment, leading to pollution and posing significant threats to wildlife and humans.[5] Despite their environmental challenges, plastics are valued for being durable, lightweight, easily transportable, and renewable in specific applications.[5] Biomass waste offers the advantages of being storable, transportable, and dispatchable. Its classification as a carbon-neutral renewable resource further enhances its appeal, making it a prime candidate for biofuel production.[6] This has prompted widespread investigation by researchers

Department of Chemical Engineering, Manipal Academy of Higher Education Manipal, Karnataka-576104, India. E-mail: ranjeet.mishra@manipal.edu

across the globe. Biomass waste has emerged as a desirable renewable biofuel source and has been extensively researched globally.[7] In China, rapeseed stalk (RS) is a crucial oil crop known for its high yield and global significance as a rich biomass resource.[8] Plastics are widely utilised in daily life due to their corrosion resistance, affordability, strong plasticity, chemical stability, lightweight nature, wear resistance, and waterproofing capabilities.[9] Annually, the agriculture sector produces about 140 billion tonnes (BT) of biomass waste globally, with only 40% utilised for fuel, feed, or power. Most of the remainder is incinerated, causing detrimental impacts on the environment and climate.[9] Similarly, 181.50 BT of lignocellulosic biomass are generated from forestry and agricultural activities, yet only 8.2 BT find practical use.

Recycling underutilised biomass into biofuels is a more sustainable alternative to landfilling or incineration and can significantly complement global renewable energy needs. Converting agricultural and lignocellulosic biomass into products like fertilisers, bioplastics, and biofuels fosters efficient resource management, reduces fossil fuel dependency, and promotes zero waste.[10] Recycling and reusing plastic waste are superior to landfilling and incineration but face limitations due to physical barriers like collection, separation, and pretreatment to remove contaminants, as well as technical challenges such as undesirable chemical reactions during processing.[11] Non-recyclable plastics, including thermosets and heavily contaminated materials, can be effectively converted into fuels or energy *via* thermochemical processes.[12] Similarly, the significant amount of underutilized biomass waste generated annually presents an opportunity to enhance global renewable energy supplies through conversion to biofuels. Processes such as pyrolysis, gasification, torrefaction, combustion, hydrothermal liquefaction, and hydrothermal carbonization are effective for transforming plastics and biomass into valuable products like char, oil, and gas.

Char is a carbon-rich, porous substance that forms by pyrolyzing biomass or biomass and plastics sources together in the absence of oxygen, resulting in a material that resists degradation. In recent years, it has garnered significant attention for its potential in various industrial and agricultural applications. The properties of char, such as its elemental composition, porosity, density, and pH, vary greatly, influencing its effectiveness for different uses.[13] Studies show that the type of material and the production process have a major impact on the characteristics of the char. Char is used in waste treatment to eliminate a range of pollutants, including organic and inorganic substances and textile dyes.[13] In agriculture, it improves soil quality by reducing nutrient loss and enhancing soil health.[14] Additionally, due to its high carbon content, char is used as a renewable fuel source for power generation. Biomass is seen as a promising renewable resource for energy, minerals, and chemicals.[15]

Pyrolysis offers several advantages over other thermochemical techniques, such as (1) lower energy consumption compared to more energy-demanding methods like gasification and hydrothermal reactions, (2) reduced emissions of harmful gases, (3) simpler scalability, and (4) portable reactors that can be relocated to different sites for flexibility.[4] As a result, co-pyrolysis of biomass and plastic waste has become an appealing option. The combination of biomass and plastics in co-pyrolysis is beneficial because (1) biomass can help alleviate the undesirable properties of plastic pyrolysis oil, such as high oxygen and moisture content, corrosivity, and viscosity, (2) plastics improve the yield and quality of bio-oil and syngas from biomass, (3) hydrogen consumption during the hydrotreatment of bio-oil is reduced, and (4) the process closes the resource loops of both biomass and plastic waste to produce biofuels.[16] The pyrolysis of plastic alone is relatively simple, but the heavy liquid phase products are often unsuitable for direct use as fuel oil. Whether plastic or biomass is pyrolyzed independently, the resulting products have several drawbacks. However, recent studies have shown that co-pyrolysis of biomass and waste plastics is a promising approach to address both environmental pollution caused by waste disposal and the generation of valuable chemicals, including liquid oils, gaseous fuels, and other high-value materials. In co-pyrolysis, biomass and plastic can be combined in various proportions and then pyrolyzed together.[17] Research has found that co-pyrolysis of plastics with lignin biomass or cellulose biomass increases gas production.[6,18] In the case of co-pyrolyzing high-density polyethylene with straw or apricot cores, nitrogen compounds in the liquid products were significantly reduced, resulting in improved oil quality.[19,20] Moreover, co-pyrolysis of lignin biomass with polypropylene (PP) decreased oxygenated compounds in the oil and produced more than 20 new aromatic compounds. During the co-pyrolysis of lignin biomass and PVC, the carbon content was significantly higher than anticipated, with a 3 : 1 mass ratio of lignin biomass to PVC yielding the highest carbon concentration.[21] Co-pyrolysis generally provides a valuable method for the development of renewable energy sources, tackling the energy crisis, and mitigating environmental pollution. Several variables influence the distribution of pyrolysis products in co-pyrolysis. Studies suggest that factors such as temperature, reaction time, biomass composition, catalyst presence, and catalyst type all play a role in determining the yield and chemical composition of pyrolysis products.[22] Among these, temperature has the most profound effect on the type and quantity of products, while reaction time primarily affects the yield of the products.[23] Additionally, co-pyrolysis of biomass with various plastics not only contributes to the production of liquid fuels and chemicals but also plays a role in environmental pollution control. The above-listed literature confirmed that all the studies are focused on the production of liquid fuel or syngas from the co-pyrolysis of biomass. However, there is a significant gap in the literature regarding the production of char from the co-pyrolysis of biomass and plastics. As a result, this study focuses on the production and characterisation of char generated through the co-pyrolysis of biomass and plastics. Notably, this is the first study to explore the conversion of plastics and biomass into char using pyrolysis techniques.

Addressing the gap in the existing literature, the present study investigates the production and characterisation of char derived from the co-pyrolysis of biomass and plastics. JCT and NRPET were pyrolyzed in a semi-batch reactor at 500 °C with

a heating rate of 10 °C min^{-1} and a nitrogen gas flow rate of 100 mL min^{-1}. The holding time was maintained at 45 min to facilitate char formation. Biomass and plastic were physically mixed in varying proportions (30%, 50%, and 80% wt%) to produce the char. Subsequently, the char was characterised based on its physical and chemical properties.

2 Materials and methods

2.1 Sample collection and preparations

Jungle Cork Tree (JCT) was brought from Basti District, Uttar Pradesh, India. However, non-recyclable polyethylene terephthalate (NRPET) (drinking water bottles) was collected from Manipal, the MIT campus. The JCT was sun-dried for 3–4 days (subjected to atmospheric conditions) and placed in a hot air oven at 105 °C overnight to remove uniform moisture content. The level of the bottle and lid was removed, and the bottle was washed with hot water and sundried dried for 3–4 days. After that, the bottle was cut into small flakes in the range of 1–1.2 cm. A cryo mill was used to make the PET flakes in powder form in the range of 850 to 750 μm. The oven-dried samples were stored in plastic bags to prevent moisture absorption.

2.2 Physicochemical characterisation feeds

Characterising the physical and chemical properties of feedstock is vital in assessing its suitability. Proximate analysis provides volatile matter (burns in the gaseous state), fixed carbon (burns in the solid state), and ash (the inorganic residue). These parameters were determined in line with ASTM-D 5142 and D1762-84 protocols. A FLASH 2000 elemental analyser (Thermo Fisher Scientific Inc., USA) was used to measure carbon (C), hydrogen (H), nitrogen (N), and sulfur (S) as per ASTM D5373, with oxygen (O) content derived by difference. The higher heating value (HHV) was determined using an oxygen bomb calorimeter (Model 1341 Plain Jacket Calorimeter). An automated titration system (Mettler Toledo pH analyzer, USA) was employed to measure the pH of the char. The biochemical analysis (cellulose, hemicellulose and lignin) was determined using NREL Laboratory Analytical Procedure,[24,25] whereas the bulk density of feeds was calculated using a measuring cylinder and digital balance.

2.3 Thermal stability analysis feeds

Thermal stability testing of the feeds and char was performed using a Thermogravimetric Analyzer (TG 209F1 Libra, Netzsch). The sample was placed in a platinum pan and heated from 300 to 900 °C at a constant heating rate of 10 °C min^{-1} under a nitrogen atmosphere. The obtained TGA and DTG data were analysed using the Universal Analysis 2000 software, version 4.5A.

2.4 FTIR analysis of feeds

Functional group analysis of the feeds and char was conducted using FTIR-ATR (IRTracer-100, Shimadzu). The spectra were recorded over a wavenumber range of 400 to 4000 cm^{-1}, with 64 scans at a resolution of 4 cm^{-1}, by placing a small sample onto the ATR crystal.

2.5 TGA-FTIR study

Gas composition analysis was conducted using a TGA-FTIR analyzer (NVENIO FT-IR spectrometer connected with TG 209F1 Libra, Netzsch). Samples of 9 ± 0.01 mg were loaded into crucibles and heated from 30 to 900 °C at 10 °C min^{-1}, with an inert gas flow of 50 mL min^{-1}. The Gram–Schmidt software was used to calculate the relative absorbance of the volatile compounds.

2.6 Pyrolysis experiment

The pyrolysis of JCT and NRPET was performed in a fixed-bed reactor made from stainless steel (SS-304) with a length of 40 cm and an inner and outer diameter of 4.5 cm and 5 cm, respectively. The reactor system consists of a nitrogen cylinder, gas rotameter, electrical furnace, control panel, condenser, and a liquid collection tank. The gas rotameter regulates the flow rate of nitrogen, while the electrical furnace is used to heat the sample in the absence of air and oxygen. The heating furnace is designed to distribute heat evenly throughout the reactor. A PID controller, connected to a K-type thermocouple, controls the reactor temperature. The control panel allows the user to adjust the temperature, heating rate, and residence time, which are directly linked to the electrical furnace. For each experiment, 100 g of sample was placed inside the reactor, and the experiment was performed at 500 °C; 10 °C min^{-1} heating rate and 100 mL min^{-1} nitrogen gas flow rate. Gases released from the reactor pass through a condenser, where they are cooled and condensed into a liquid, which is stored in a glass container. It is important to note that the gas flow is initiated 10 min before the experiment to eliminate any contamination from the reactor. Nitrogen gas is supplied from the bottom inlet of the reactor. A schematic diagram of the reactor is provided in Fig. 1.

Finally, the yield of biocarbon was calculated using the eqn (1).

$$\%\ \text{Yield of biocarbon} = \left[\frac{\text{solid material left after the pyrolysis}}{\text{weight of original pyrolytic oil}}\right] \times 100 \quad (1)$$

2.7 Optimization of temperatures

Temperature optimisation is crucial for enhancing process efficiency, yield, and product quality in pyrolysis or chemical reactions. It involves determining the ideal temperature range that maximises desired product formation while minimising unwanted byproducts. Achieving optimal temperatures requires balancing reaction rates and thermal stability to ensure energy efficiency and consistent, high-quality output. In this study, three different temperatures (400, 450, 500, 550 and 600 °C) were selected at 10 °C min^{-1} heating rate and 100 mL min^{-1} inert gas flow rate. The holding time for all the tests was kept at 45 min. Also, NRPET was loaded into different proportions (30, 50 and 80 wt%) to study the effect of plastics on the char properties and yield.

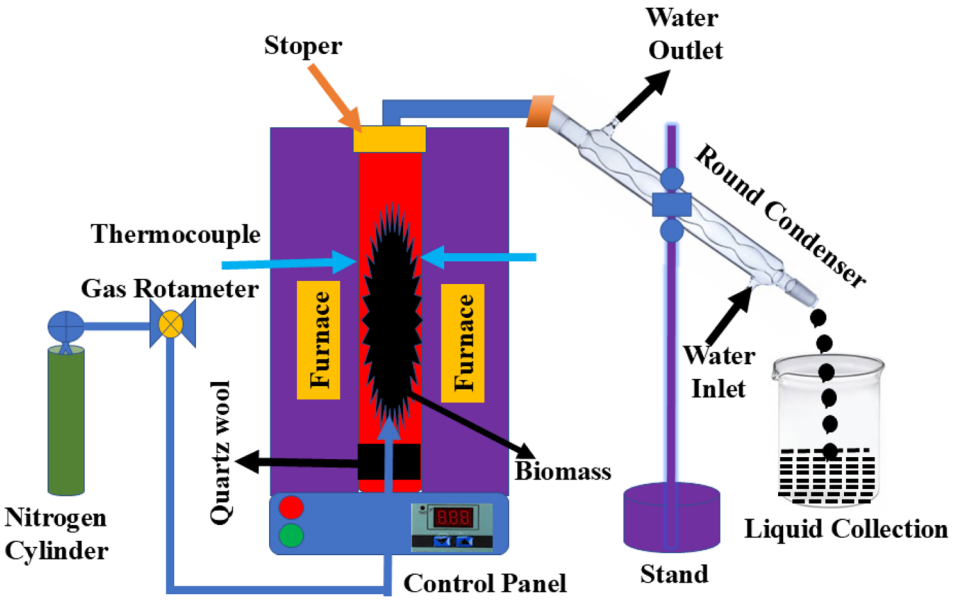

Fig. 1 Schematic arrangement of the pyrolysis experimental setup of the pyrolysis.

2.8 Characterization of char

Char was obtained from each experiment and milled for 2 h at 180 rpm in a planetary ball mill (QXQM-2, TENCAN) using grinding balls. The milled samples were then carefully collected and stored in airtight bags to avoid moisture absorption before further analysis. The proximate analysis (moisture content and ash content), elemental analysis, HHV, and bulk density were performed as per the method described in Section 2.2. The pH meter was calibrated using buffer solutions at pH levels of 4, 7, and 10. A sample of 1 g of dry char was combined with 50 mL of distilled water and mixed well. The solution was then stirred overnight at 25 °C to ensure consistency before measuring the pH. BET surface area measurements of char were conducted using a Brunauer–Emmett–Teller analyzer (Quantachrome, Autosorb-IQ MP) and ASiQwin 5 software. To eliminate moisture, the dried char was degassed at 200 °C for 3 h before being placed in the analyser. The sample was evaluated by adsorption/desorption analysis following ASTM standard D6556-19 for multi-point BET. An Autolab PGSTAT302N (Netherlands) was used to determine the electrical conductivity of char. Char had been ball-milled for 2 h and placed in a hollow cylinder. A piston weighing 3 kg was gently placed on top, allowing for 20–30 s of natural compaction. Electrodes were attached to both ends of the cylinder and connected to the analyser for conductivity measurement.

2.9 Raman and scanning electron microscopy analysis

Char samples were analysed with a Raman spectrometer (Horiba Jobin Vyon, Model LabRam HR) utilising a 785 nm laser at 200 mW. Raman spectroscopy determined the ratio of graphitic to disordered carbon, with settings adjusted to 10× zoom and a 50 μm slit for precision. Furthermore, char particle size and morphology at multiple temperatures were studied with a Scanning Electron Microscope (SEM) (Zeiss, Sigma) coupled with Energy-Dispersive Spectroscopy (EDS). The SEM imaging was conducted at an accelerating voltage of 5 kV.

3 Results and discussions

3.1 Physicochemical characterization of biomass and plastics

Biomass characterisation is crucial before pyrolysis as it helps determine the material's chemical composition, moisture content, and volatile matter. These properties influence the pyrolysis process, affecting yield, energy efficiency, and product quality. Understanding biomass ensures optimised pyrolysis conditions, enhancing the production of valuable biofuels and chemicals. The physicochemical study of JCT and NRPET were characterised and matched with the published literature, such as in pine sawdust and Sal sawdust,[26] deodar sawdust,[27] polypropylene (PP), high-density polyethylene (HDPE),[28] and listed in Table 1. The proximate analysis of JCT and NRPET confirmed 7.23% moisture content, 75.20 and 89.18% volatile matter, 3.67 and 2.07% ash content, and 13.90 and 8.75% fixed carbon, respectively. The moisture content of JCT was found to be below the threshold limit (<10%), suggesting suitable feeds for pyrolysis. Further, the volatile matter of JCB was found to be in the same range as SW, PW, and DS, whereas NRPET was also found to be in the same range as PP and HDPE (Table 1). Volatile matter and moisture content significantly affect the pyrolysis process. Volatile matter, which includes gases and low-molecular-weight compounds, influences the formation of bio-oil and syngas during pyrolysis.[27] Higher volatile content generally leads to higher liquid yield and more gaseous products. Moisture content, on the other hand, must be minimised before pyrolysis as it consumes energy to evaporate during the process, lowering efficiency and potentially hindering the

Table 1 Physicochemical studies of JCT and NRPET were compared with the published literature

Analysis	Jungle cork tree (JCT)	Non-recyclable polyethylene terephthalate (NRPET)	Sal sawdust (SW)[26]	Pine sawdust (PW)[26]	Deodar sawdust (DS)[27]	Polypropylene (PP)[28]	HDPE[28]
Proximate analysis (wt%) on dry basis							
Moisture	7.23 ± 0.80	—	8.88	6.09	3.07	0.44	0.32
Volatile matter	75.20 ± 1.1	89.18 ± 1.1	76.30	78.30	80.87	93.84	91.88
Ash content	3.67 ± 0.40	2.07 ± 0.20	1.14	2.07	3.35	3.68	3.90
Fixed carbon	13.90 ± 0.80	8.75 ± 0.30	14.90	12.16	12.68	2.04	3.90
Elemental analysis (wt%) on dry basis							
C	49.12 ± 0.60	64.12 ± 0.60	49.83	50.30	46.09	83.28	83.40
H	8.24 ± 0.20	5.02 ± 0.20	6.09	6.00	7.02	13.81	12.71
O	40.30 ± 1.20	30.86 ± 1.20	43.56	42.99	46.39	2.90	3.80
N	1.65 ± 0.08	—	0.58	0.69	0.50	0.01	0.08
S	0.69 ± 0.02	—	—	—	—	0.00	0.002
O/C	0.62	0.36	0.66	0.46	0.75	—	—
H/C	2.01	0.94	1.47	1.43	1.83	—	—
Higher heating value (MJ kg^{-1})	22.55 ± 1.2	38.56 ± 1.6	18.20	18.44	18.67	44.43	46.48
Bulk density (kg m^{-3})	367.26 ± 1.2	281.67 ± 1.2	321.91	296.27	—	—	—
Biochemical analysis (wt%)							
Hemicellulose	23.56	—	14.59	15.35	—	—	—
Cellulose	41.60	—	52.36	55.92	—	—	—
Lignin	10.81	—	11.18	10.55	—	—	—

formation of desired products.[27] The excess moisture can also cause temperature fluctuations and incomplete thermal decomposition, reducing char yield and affecting product consistency. Therefore, controlling both factors is essential for optimising pyrolysis outcomes.[27] The ash content of JCVT was found to be higher than PW and SW, whereas NRPET was found to be in the same range as PP and HDPE. The fixed carbon of JCT was found to be in the same range as PW, SW, and DS, whereas NRPET was found to be higher than that of PP and HDPE. Ash content and fixed carbon play crucial roles in pyrolysis. Ash content does not contribute to energy production but can affect the reactor efficiency and cause operational issues.[27] Fixed carbon contributes to char production and energy output, influencing the overall yield and quality of pyrolysis products. In addition, higher fixed carbon enhances char stability and energy content.[27] The elemental analysis of JCT and NRPET confirmed 49.12 and 64.12% carbon, 8.24 and 5.20% hydrogen content, 40.30 and 30.86% oxygen content, and the significance of nitrogen and sulphur compounds. The elemental composition of JCT and NRPET was found to be close to the value reported for PW, SW, DS, PP and HDPE. The carbon, hydrogen, and oxygen content in biomass are vital factors in pyrolysis, as they determine the composition and quality of the resulting products. Carbon content influences the yield and stability of char, with higher carbon content leading to a more stable and energy-dense char. Hydrogen plays a critical role in the formation of bio-oil and syngas during pyrolysis. A higher hydrogen content favours bio-oil production, which is rich in hydrocarbons, while excessive hydrogen can lead to more gaseous products like methane. Oxygen content in biomass is significant as it can affect the thermal decomposition process. A higher oxygen content can lead to the formation of more oxygenated compounds, reducing the energy yield and lowering the quality of bio-oil. Proper balance between these elements optimises the pyrolysis process, ensuring the production of valuable biofuels, char, and gases while minimising unwanted by-products and energy losses. Nitrogen and sulphur content in biomass affect pyrolysis by producing harmful compounds like ammonia, nitrogen oxides, and sulphur dioxide. These emissions degrade product quality, pose environmental risks, and can damage catalysts. Controlling nitrogen and sulphur helps reduce pollution, improve bio-oil quality, and ensure cleaner pyrolysis processes. The O/C (oxygen-to-carbon) and H/C (hydrogen-to-carbon) ratios are crucial in pyrolysis as they influence the composition of pyrolysis products. A lower O/C ratio enhances char yield and energy density, while a higher H/C ratio favours bio-oil production, improving the quality of liquid fuels and gases. The molar ratio of O/C and H/C was printed using the Van–Krevelen diagram and listed in Fig. 2. From Table 1, it was found that the O/C value for JCT and NRPET was found to be lower, and the value of H/C was found to be higher suggesting utilisation JCT and NRPET can be used for pyrolysis feedstock. Furthermore, the HHV of JCT was found to be 22.55 MJ kg^{-1}, which is slightly higher than that of PW, SW, and DS. HHV of NRPET was found to be 38.56 MJ kg^{-1}, which is slightly lower than the value reported for PP and HDPE. Furthermore, the bulk density of JCT and NRPET was found to be 367.26 and 281 367 kg m^{-3}, which shows that storage and

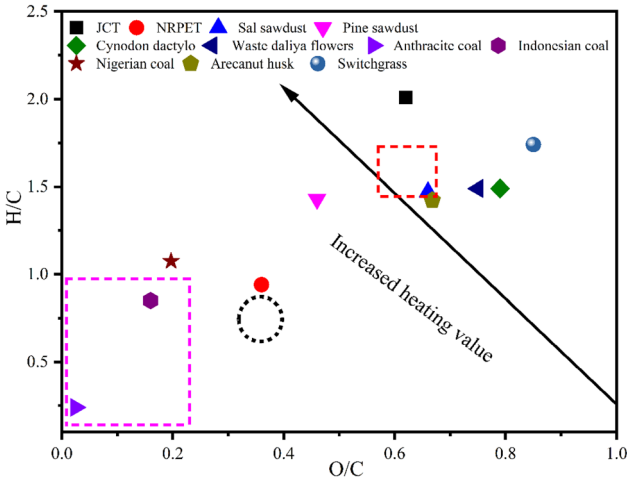

Fig. 2 Van–Krevelen diagram of different types of char and coal chars.

transportation would be easier. Higher heating value (HHV) determines the energy content of the pyrolysis products, with higher values indicating more efficient energy recovery. Bulk density influences feedstock handling and reactor performance, as denser materials improve heat transfer and reduce reactor volume requirements. Finally, cellulose, hemicellulose and lignin were found to be 41.60, 23.56 and 10.81%, respectively. The value reported for JCT was found to be lower than that of PW and SW. Cellulose, hemicellulose, and lignin are key components of biomass that influence pyrolysis. Cellulose and hemicellulose decompose at lower temperatures, producing more volatile products like bio-oil. Lignin, being more thermally stable, yields more char and gases. Their relative content affects product distribution and pyrolysis efficiency.

3.2 TGA-FTIR analysis of feeds

TGA-FTIR facilitates the analysis of volatiles emitted during pyrolysis, enabling the assessment of gases such as hydrogen, methane, carbon dioxide, and carbon monoxide with significant ecological effects.[29] Fig. 3a–e displays the 3D surface plots for JCT, NRPET, and their blends (JCT + NRPET 30, 50 and 80%). Meanwhile, the relative amounts of volatile gases released during material heating were also listed on the right side. Volatile products were primarily released between 15–44 min. TGA-FTIR analysis showed that JCT, NRPET, and their blends (30%, 50%, and 80%) generated varying volatiles due to differences in chemical makeup. The 3D surface plots of JCT, NRPET, and their blends (30%, 50%, and 80%) exhibited a similar pattern, with noticeable differences in the CO and CO_2 peaks. These differences resulted from decarboxylation reactions occurring during pyrolysis, which promoted CO_2 formation by removing a carbon atom from the carbon chain.[29] The peaks at 3485 and 3573 cm^{-1} were linked to the presence of moisture and alcohol, while those at 2932 and 2930 cm^{-1} indicated the release of hydrocarbons.[30] Peaks at 1768, 1721, 1725, and 1769 cm^{-1} confirmed the emission of carbonyl compounds, and peaks at 2362 and 2366 cm^{-1}, attributed to asymmetric vibrations, confirmed the presence of carbon dioxide.[31] Additionally, peaks at 1113 and 1129 cm^{-1}, associated with C–O stretching, signified the release of ethers during pyrolysis.[30,31] The pyrolysis of JCT, NRPET, and their blends (30%, 50%, and 80%) revealed that most of the hot volatiles generated were predominantly hydrocarbons. This is consistent with the feed composition, which includes various hydrocarbons such as alkanes, alkenes, alkynes, cycloalkanes, and alkadienes. Among JCT and NRPET, NRPET has maximum hydrocarbons as plastic is made from carbon and hydrogen.[31] It was also found that JCT releases a maximum amount of CO_2 as compared to NRPET and their blends (30%, 50%, and 80%). Biomass pyrolysis generally releases higher amounts of CO_2 compared to plastic pyrolysis due to the chemical composition of the feedstocks. Biomass, primarily composed of lignocellulosic materials (cellulose, hemicellulose, and lignin), contains a significant amount of oxygen. During pyrolysis, this oxygen is released in the form of CO_2 as the organic components break down. The high oxygen content in biomass, combined with the decarboxylation reactions that occur during pyrolysis, leads to substantial CO_2 emissions. On the other hand, plastics like polyethylene have a much lower oxygen content. These materials are composed mainly of carbon and hydrogen, and their pyrolysis produces primarily hydrocarbons (such as alkanes, alkenes, and other gaseous products) rather than CO_2.[32] The lower oxygen content in plastics means there are fewer opportunities for decarboxylation reactions, which results in lower CO_2 production during pyrolysis. Moreover, the structure and composition of plastics allow for the formation of valuable liquid fuels and gases, such as methane, ethylene, and propylene, rather than primarily carbon dioxide. This difference in chemical makeup between biomass and plastics contributes to the varying levels of CO_2 emissions during their pyrolysis processes. Carbonyl groups (carboxylic acids, ketones, aldehyde, and amide) and CO were found to be other predominant compounds released during the pyrolysis of biomass. Biomass pyrolysis releases more CO and carbonyl compounds due to its higher oxygen content, which leads to decarboxylation and breakdown of oxygenated groups like aldehydes and ketones. In contrast, plastics with lower oxygen content primarily produce hydrocarbons, resulting in lower CO and carbonyl compound emissions during pyrolysis.[32] The alcohol and moisture content were also found in hot volatiles of JCT. However, moisture content was found in plastic pyrolysis. It was observed that many gases released during pyrolysis consisted of hydrocarbons, carbonyl compounds, ethers, CO, and CO_2, with smaller amounts of water and alcohol. The gases that evolved during pyrolysis were significantly influenced by the particle size of the material.[32] Further, it was noticed that blending of NRPET at 30, 50 and 80 wt% with JCT significantly increased the hydrocarbons and reduced the formation of CO, CO_2 and oxygenated compounds compared to JCT. Further, the maximum hydrocarbon was found in NRPET and 80% blend ratio compared to all ratios. The addition of plastics helps to add hydrocarbons to hot volatiles and reduces the formation of CO, CO_2, and other oxygenated compounds. Moreover, the addition of plastics with biomass significantly increases the number of pyrolysis products such as char.

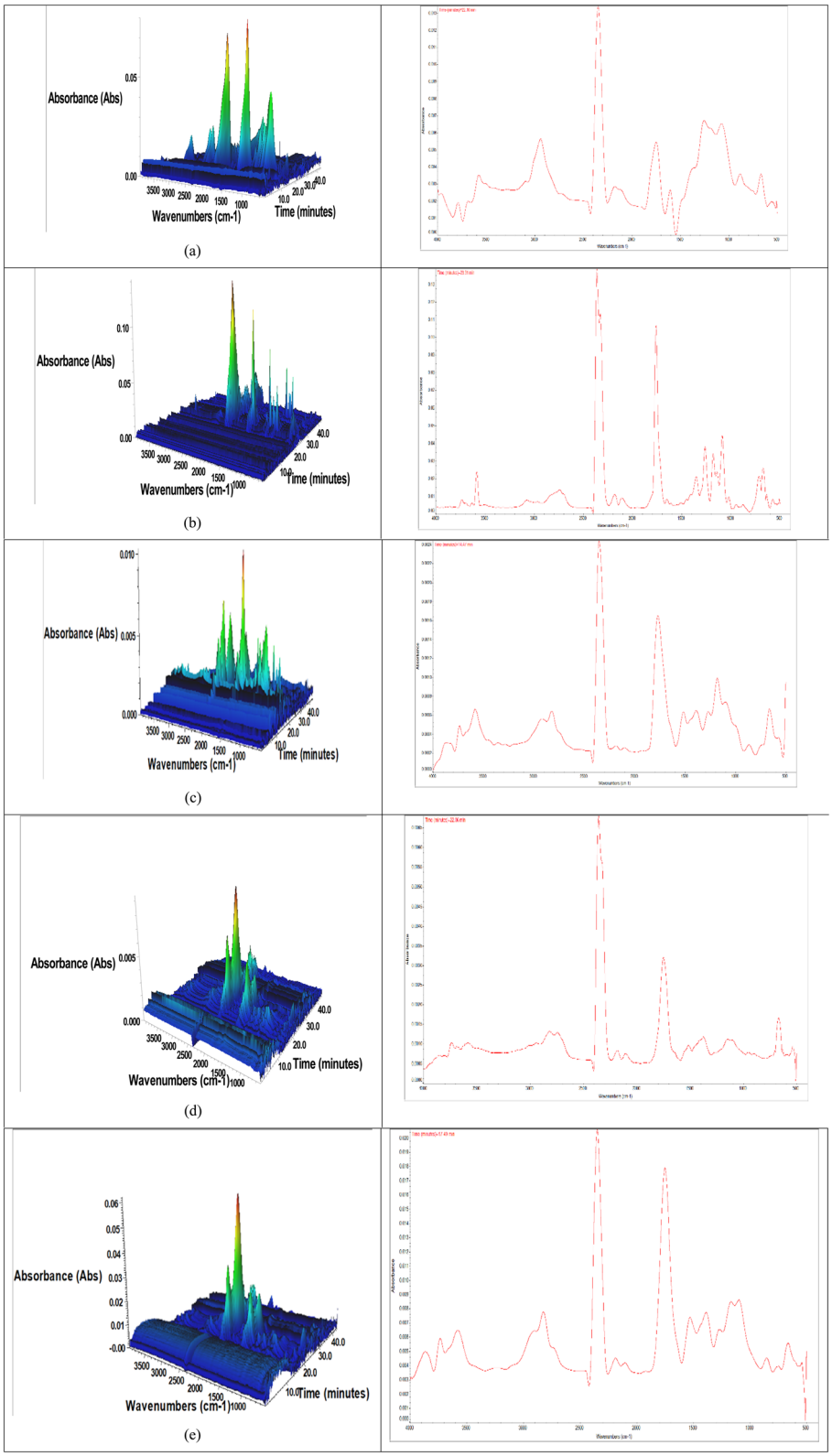

Fig. 3 TGA-FTIR analyser of (a) JCT, (b) NRPET (c) JCT + NRPET (30 wt%), (d) JCT + NRPET (50 wt%) and (e) JCT + NRPET (80 wt%).

3.3 Thermal stability and FTIR study of feeds

The thermal stability profile of JCT and NRPET is presented in Fig. 4. The thermal decomposition profile of JCT confirmed three decomposition stages (drying stage from 30–150 °C, active pyrolysis stage from 150–550 °C and passive pyrolysis stage at >550 °C) whereas NRPET has single stage decomposition on the temperature range of 350–550 °C. The first stage involved the

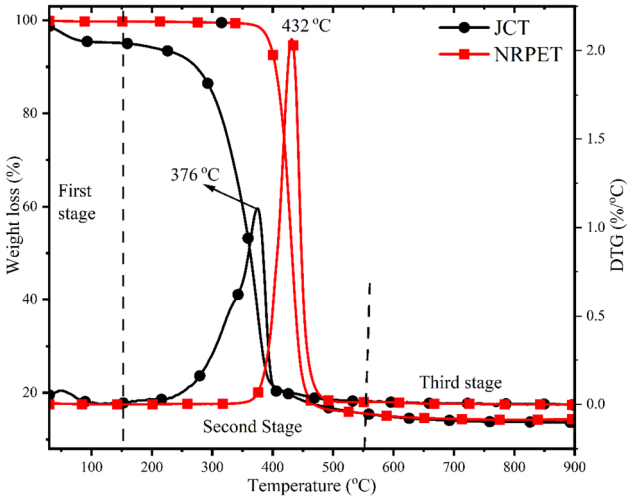

Fig. 4 Thermal stability analysis of JCT and NRPET at 10 °C min^{-1} heating rate.

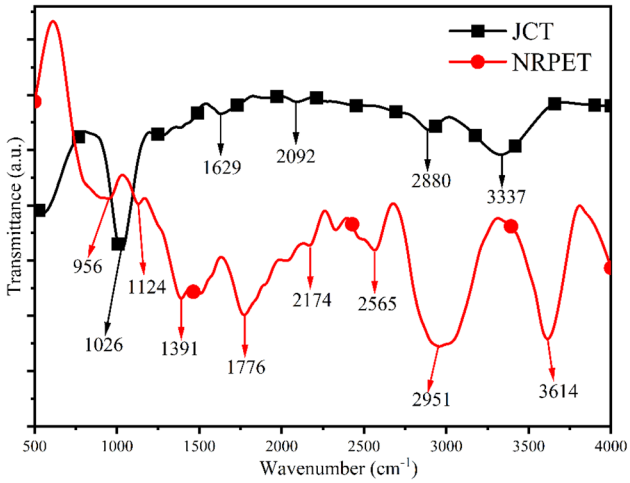

Fig. 5 FTIR analysis of JCT and NRPET.

decomposition of light volatile matter and unbounded moisture content. The second stage involved the decomposition of biomass constituents (cellulose and hemicellulose in smaller molecules) in JCT and polymer structures into smaller molecules in NRPET. In biomass pyrolysis, cellulose decomposes primarily between 300–400 °C, breaking down into volatile compounds and producing gases, tar, and char. Hemicellulose decomposes earlier, around 200–300 °C, yielding primarily acetic acid, carbon dioxide, and other volatiles. This early decomposition of hemicellulose and later breakdown of cellulose influence the yield and composition of pyrolysis products. Finally, at the final stage, lignin decomposed at a higher temperature at a slower rate due to the presence of aromatics or derivatives of aromatics compounds. DTG thermograph shows a distinct peak around 60 °C, indicating the removal of moisture and light volatile matter, accounting for approximately 4.91% mass loss. This initial stage reflects dehydration and volatilization of low-molecular-weight compounds, preparing the biomass for subsequent thermal decomposition of its main components. A prominent second peak at 376 and 432 °C on the DTG thermograph confirms the decomposition of cellulose and polymer structure with significant mass losses of approximately 79.57% for JCT and 83.81% for NEPET. This stage reflects the thermal breakdown of cellulose into volatile gases, bio-oil, and residual char, representing the major degradation phase of biomass. The volatile matter reported for JCT and NRPET in Table 1 also supports the decomposition percentage in the second stage. Finally, the decomposition of the lignin did not have any sharper peak and accounted for 2% decomposition due to a slower decomposition rate at a wide temperature range.

3.4 FTIR analysis of feeds

Fig. 5 presents the FTIR spectrum of JCT and NRPET, covering the range 500–4000 cm^{-1}, revealing several functional groups. The broad band at 3337 cm^{-1}, due to –OH stretching, indicates water, acids, phenols, and aromatics.[33] A C–H stretching peak at 2880 cm^{-1} suggests alkane presence, while the C=O stretching band at 2092 cm^{-1} points to carbonyl and carboxylic acids.[33] The 1629 cm^{-1} band, related to C–H stretching in methyl groups, suggests cellulose and hemicellulose.[34] The 1026 cm^{-1} peak, attributed to C–O stretching, reflects cellulose, hemicellulose, and lignin.[28] Peak below 950 cm^{-1} confirmed the presence of poly and mono aromatics compounds.[34] In NRPET, the peaks at 3614 cm^{-1}, 1391 cm^{-1}, and 956 cm^{-1} indicate aromatic and substituted phenyl rings.[28] Peaks at 2174 cm^{-1} and 2526 cm^{-1} show C=C stretching for carbon double bonds, while the 2951 cm^{-1} peak from C–H stretching suggests $-CH_3$ or $-CH_2-$ groups.[28] Additionally, peaks at 1776 cm^{-1}, and 1124 cm^{-1}, linked to C–H vibrations, confirm aromatic structures.[34]

3.5 Optimization of temperatures

Optimising temperatures in pyrolysis is essential for maximising the yield and quality of products like bio-oil, gas, and char. Lower temperatures favour char, while higher

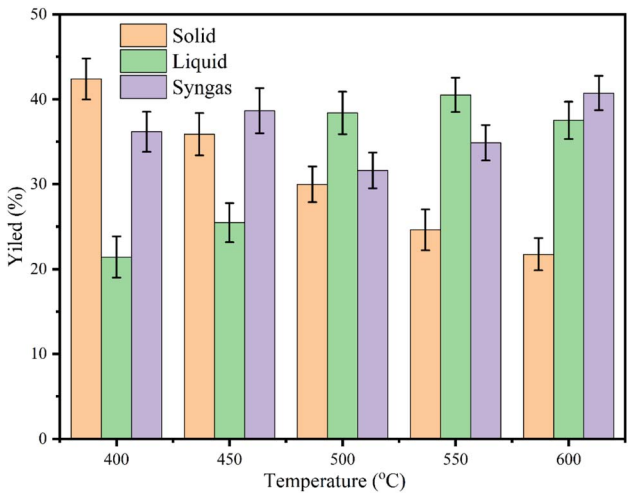

Fig. 6 Optimization of pyrolytic product yield with varying temperatures.

temperatures enhance bio-oil and gas production. Precise temperature control improves reaction rates, product distribution, and energy efficiency, tailoring outputs to specific applications. Although at lower temperatures, the yield of char is higher, the quality of char is lower; thus, the present study used 500 °C, 10 C min^{-1} heating rate, 100 mL min^{-1} of nitrogen gas flow rate and 45 min holding time. The results confirmed 42.40, 35.89, 29.98, 24.60, 21.74% char, 21.42,25.46, 38.40, 40.52, 37.52% liquid, and 36.18, 38.65, 31.5, 34.85, 40.74% syngas from 400, 450, 500, 550 and 600 °C. From Fig. 6, it was noticed that by increasing temperature from 400–600 °C, the yield of char decreased, whereas the yield of syngas and liquid was increased. Increasing the pyrolysis temperature from 400–600 °C accelerates the breakdown of biomass, promoting greater thermal decomposition. This process converts more solid biomass (char) into volatile compounds, increasing the yield of gas and bio-oil (liquid). Higher temperatures enhance cracking reactions and volatilization, which reduces char formation while favouring gas and liquid products. It was found that at 400 °C, the yield of char was higher (42.40%), and at 600 °C, the char yield was lower (21.74%). At 400 °C, the biomass undergoes slower decomposition, resulting in a higher yield of char as fewer volatiles are released. However, at 600 °C, increased thermal energy drives extensive breakdown of solid biomass into volatile compounds, reducing char yield and boosting the production of gas and liquid products. Similar patterns in char, liquid and syngas were noticed at 450 and 550 °C. The char yield at 500 °C was found to be ~30%, which is lower than 400 and 450 °C still used in this study due to improved properties of char.

3.6 Physicochemical characterization of char

The characterisation results of JCT, NRPET, JCTB + NRPET (30 wt%), JCTB + NRPET (50 wt%) and JCTB + NRPET (80 wt%) are listed in Table 2. The yield of JCTB, NRPET, JCTB + NRPET (30 wt%), JCTB + NRPET (50 wt%) and JCTB + NRPET (80 wt%) were found to be 29.28, 14.19, 24.71, 20.91 and 17.51%, respectively. It was found that by blending NRPET at 30, 50 and 80% with JCT, the yield of char was reduced by 5.27, 9.07 and 12.47%, respectively. The blending of plastics with lignocellulosic biomass in pyrolysis reduces char yield because plastics, primarily made of hydrocarbons, promote decomposition at higher temperatures, which accelerates the breakdown of biomass into volatiles. This blend facilitates thermal cracking and synergistic reactions that convert more solid material into liquid and gaseous products. Consequently, less char is formed as more biomass and plastic are transformed into bio-oil and gas through these intensified reactions.[35] The proximate analysis confirmed 4.46 and 0.50% moisture content and 3.42 and 1.96% ash content in JCT and NRPET, respectively. Further, it was noticed that blending NRPET with JCT at 30, 50 and 80 wt% reduced the moisture and ash content. Blending plastic with lignocellulosic biomass reduces moisture and ash content because plastics dilute the biomass's moisture and ash components, resulting in lower moisture content. This blend yields a cleaner pyrolysis process, with reduced ash and a higher proportion of volatile-rich products like bio-oil and gas.[36] Furthermore, the elemental composition of JCT and NRPET was found to be 66.31 and 90.91% carbon, 7.46 and 4.80% hydrogen, 23.65 and 3.38% oxygen, 2.11 and 0.80% nitrogen content in char. The NRPETB has a higher carbon content (90.91%) than JCT (66.31%), as plastics are mainly made of hydrocarbons. However, by blending NRPET at 30, 50 and 80 wt%, the carbon content of char was increased by 7.77%, 14.74% and 22.59%, respectively. Blending plastic with lignocellulosic biomass increases the carbon content of char because plastics, being rich in carbon, contribute more to char formation during pyrolysis. This leads to a higher carbon

Table 2 Physicochemical characterisation of JCTB, NRPETB with different proportions

Sample name	JCTB	NRPETB	JCTB + NRPET (30 wt%)	JCTB + NRPET (50 wt%)	JCTB + NRPET (80 wt%)
Yield (wt%)	29.98 ± 0.10	14.19 ± 0.70	24.71 ± 0.24	20.91 ± 0.12	17.51 ± 0.04
Proximate analysis (wt%)					
Moisture	4.46 ± 0.23	0.5 ± 0.002	3.26 ± 0.01	2.98 ± 0.06	2.18 ± 0.10
Ash content	3.42 ± 0.50	1.96 ± 0.08	2.08 ± 0.22	2.57 ± 0.15	2.62 ± 0.37
Elemental analysis (wt%)					
C	66.31 ± 0.027	90.91 ± 0.024	74.08 ± 0.040	81.05 ± 0.02	88.90 ± 0.42
H	7.46 ± 0.040	4.80 ± 0.06	7.51 ± 0.02	6.90 ± 0.04	4.65 ± 0.04
O	23.65 ± 0.012	3.38 ± 0.009	16.68 ± 0.14	10.71 ± 0.09	5.6 ± 0.09
N	2.11 ± 0.014	0.80 ± 0.02	1.26 ± 0.011	1.02 ± 0.009	0.85 ± 0.012
S	0.56 ± 0.004	—	0.47 ± 0.007	0.32 ± 0.004	—
O/C	0.27	0.028	0.17	0.099	0.047
H/C	1.35	0.64	1.22	1.02	0.63
HHV (MJ kg^{-1})	29.48 ± 1.6	36.86 ± 1.4	33.16 ± 1.4	35.49 ± 1.1	35.65 ± 1.1
Bulk density (kg m^{-3})	244.12 ± 1.5	633.09 ± 1.1	389.63 ± 1.1	416.56 ± 1.2	444.23 ± 0.60
BET surface area (m^2 g^{-1})	62.36 ± 1.8	4.36 ± 0.20	52.35 ± 1.2	38 ± 0.88	31.58 ± 0.11
pH	5.23 ± 0.4	1.25 ± 0.6	4.16 ± 0.6	2.16 ± 0.6	1 ± 0.1
Electrical conductivity (S m^{-1})	0.009743 ± 0.00030	0.01231 ± 0.00054	0.01099 ± 0.00046	0.008227 ± 0.00038	0.007855 ± 0.00012

concentration in the final char product compared to pure biomass pyrolysis.[37] Further, the hydrogen content of char was found to be reduced by blending of NRPET at 30, 50 and 80%. Blending plastic with lignocellulosic biomass reduces the hydrogen content of char because plastics, predominantly composed of carbon, have lower hydrogen content compared to biomass. This dilutes the hydrogen-rich components in the char, resulting in a lower hydrogen content.[38] The oxygen content of char was found to be decreased by blending of NRPET because NRPET has low oxygen, reducing the overall oxygen composition.[39] The nitrogen and sulphur content of char was also found to be decreased by blending NRPET with JCT because NRPET contains minimal nitrogen and sulphur compounds. The H/C and O/C ratios of char indicate their stability, aromaticity, and carbonisation level. A lower H/C ratio suggests higher aromaticity and thermal stability, making char more resistant to decomposition. A lower O/C ratio implies reduced polarity and greater hydrophobicity, enhancing the suitability of char for carbon sequestration and soil amendment.[40] The results of the O/C ratio of JCTB and NRPETB JCTB + NRPET (30 wt%), JCTB + NRPET (50 wt%) and JCTB + NRPET (80 wt%) were found to be reduced by blending plastic with biomass which suggested a reduced polarity and greater hydrophobicity of char for carbon sequestration and soil amendment.[40] Further, the H/C ratio of JCT was found to be higher than NRPET, along with the other blending ratios, confirming slightly lower stability, aromaticity, and carbonisation level.[40] HHV of char was found to be increased by blending NRPET with JCT by 3.68, 6.01 and 6.17 MJ kg^{-1}, respectively. Plastics blending with biomass increases the higher heating value (HHV) of char because plastics are rich in carbon and hydrogen, which contribute to higher energy content. This results in a char with enhanced calorific value, making it more efficient as a fuel.[41] The bulk density of JCTB was found to be lower than NRPETB. However, char obtained by blending NRPET with JCT was found to be increased. Char derived from plastic pyrolysis has a higher bulk density than biomass-derived char due to the compact plastic, carbon-rich structure. During pyrolysis, plastics yield denser, less porous char with fewer voids, resulting in a greater mass per unit volume compared to biomass char.[41] The BET surface area analysis confirmed that blending NRPET with JCT at different proportions leads to a reduced surface area. Blending plastics with biomass decreases the BET surface area of char because plastics produce a denser, less porous structure during pyrolysis. This limits the formation of micropores compared to biomass, resulting in char with a lower overall surface area for adsorption applications.[41] The pH of the JCTB was found to be higher than NRPET, whereas blending of NRPET with JCT again reduced the pH of the char but was higher than the NRPETB. Finally, the electrical conductivity of JCTB was found to be lower than that of NRPETB. However, the electrical conductivity of char was found to be increased by blending plastics with biomass. Blending plastics with biomass increases the electrical conductivity of char because plastics, particularly those with conductive additives or carbon-rich structures, contribute to a higher carbonisation level during pyrolysis. This leads to more conductive carbon structures and interconnected networks within the char, enhancing its conductivity.[42,43]

3.7 Thermal stability and FTIR analysis of char

The thermal stability profile of JCTB, NRPETB, JCTB + NRPETB (30 wt%), JCTB + NRPETB (50 wt%), and JCTB + NRPETB (80 wt%) was listed in Fig. 7a and b. From the TG profile of char, it was noticed that NRPETB has a high thermal stability profile, which decomposed around 5.47%. However, JCTB was found to have lower thermal stability, which decomposed 43.38%. The char derived from the plastics pyrolysis has pure carbon and is compact, thus improving the thermal profile of char. The char derived from biomass pyrolysis has many impurities, such as indigested biomass, which decreases the thermal stability of the char.[44] Further, it was found that the blending of NRPET with JCT improved the thermal stability profile of char. It was found that 8.69, 8.37 and 7.56% decomposition was taken in the case of JCTB + NRPETB (30 wt%), JCTB + NRPETB (50 wt%), and JCTB + NRPETB (80 wt%). As we increased the plastic loading

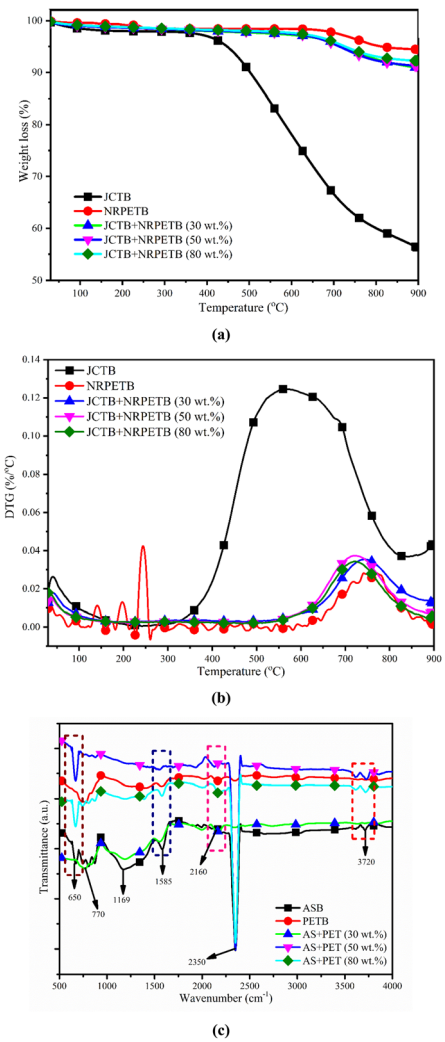

Fig. 7 Thermal stability analysis of char at 10 °C min^{-1} heating rate (a) TGA profile, (b) DTG profile, and (c) functional group analysis of char.

with biomass, the thermal stability of char improved due to the pure form of char. DTG thermograph of char confirmed that the minimum rate of decomposition (0.124 °C min^{-1}) happened in JCTB char due to lower thermal stability. However, the minimum rate of decomposition (0.0.028 °C min^{-1}) was taken for NRPETB char due to the higher thermal stability of char. Further, the decomposition rate was found to be 0.037, 0.035, 0.034 °C min^{-1} for JCTB + NRPETB (30 wt%), JCTB + NRPETB (50 wt%), and JCTB + NRPETB (80 wt%). It is worth mentioning

Table 3 Value of I_D/I_G ratio of char

Sample name	I_D/I_G ratio
JCTB	0.8616
NRPETB	0.8563
JCTB + NRPETB (30 wt%)	0.8566
JCTB + NRPETB (50 wt%)	0.8576
JCTB + NRPETB (80 wt%)	0.8575

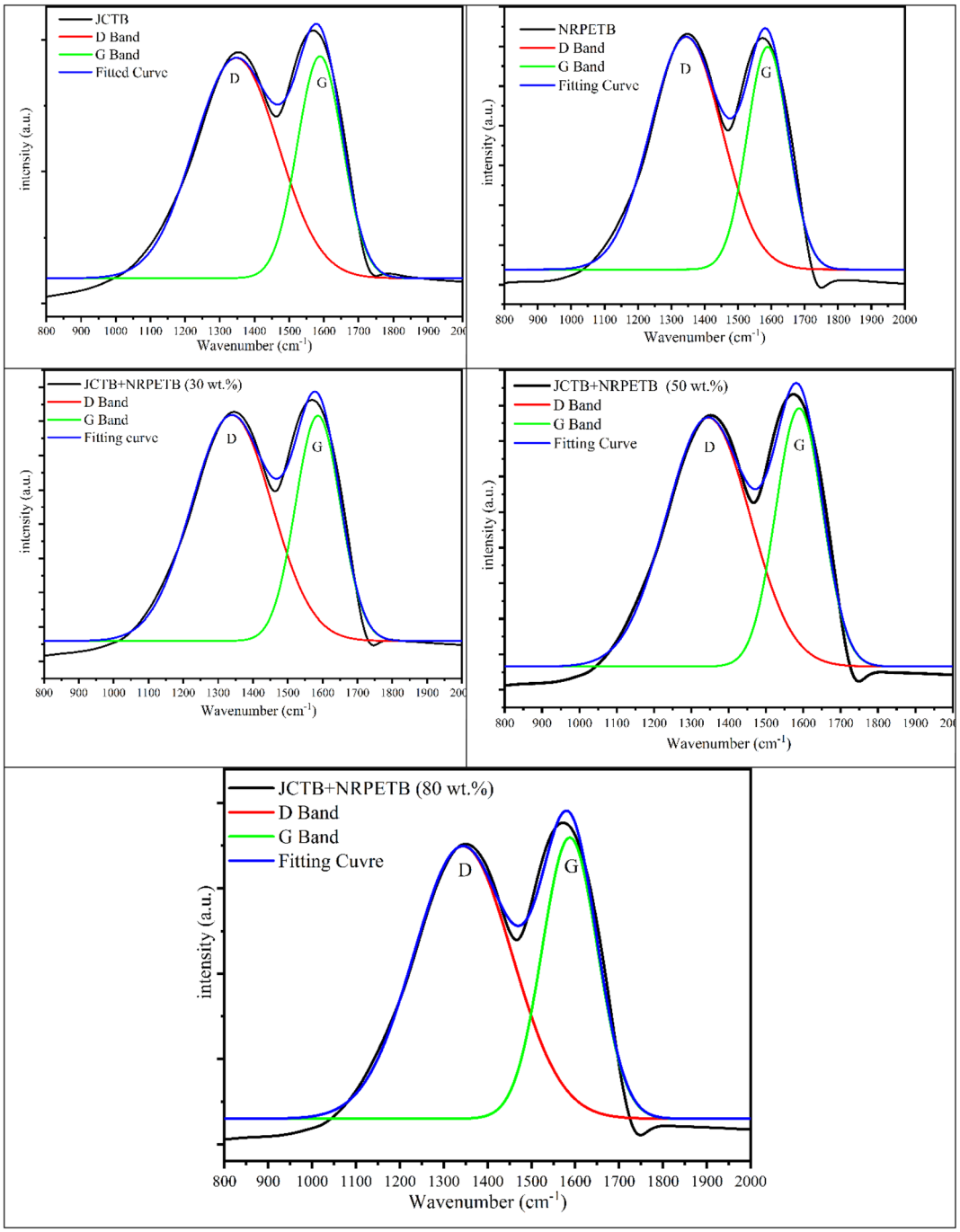

Fig. 8 Raman analysis of char derived at 500 °C.

that the DTG profile has a noisy curve due to the loss decomposition of char.

The functional group analysis of char was performed using an FTIR analyser and presented in Fig. 7c. The IR band peak of 3720 cm^{-1} confirmed Free O–H stretching of phenolic and alcoholic –OH.[45] The peak 2350 cm^{-1} attributed to symmetric C–H stretching confirmed aliphatic CH_x in char.[45] The peak 2160 cm^{-1} related to C=C stretching and C=O stretching

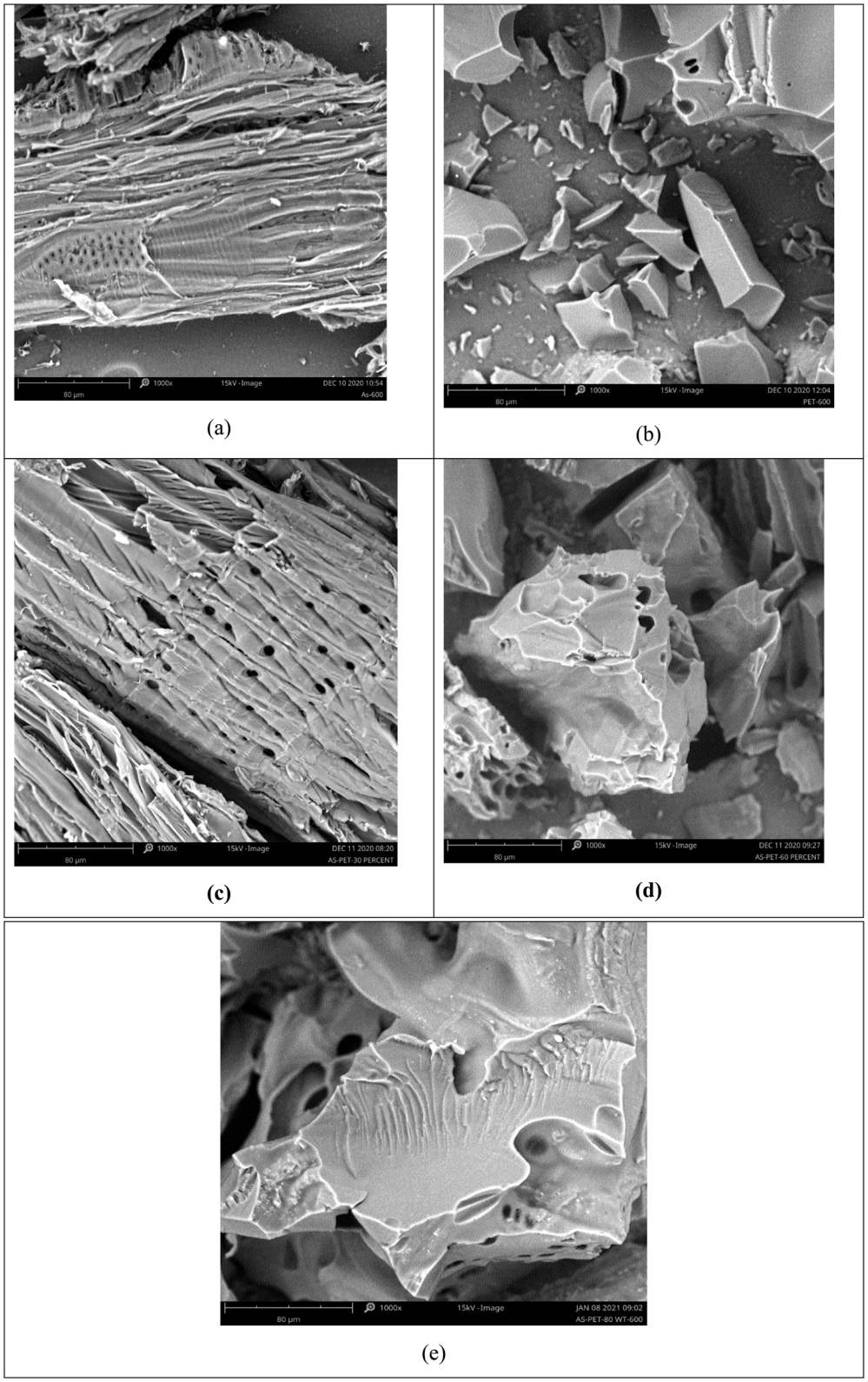

Fig. 9 SEM analysis of (a) JCTB, (b) NRPETB, (c) JCTB + NRPETB (30 wt%), (d) JCTB + NRPETB (50 wt%) and (e) JCTB + NRPETB (80 wt%).

pointed aromatic components and conjugated ketones.[45] Further peak 1585 cm^{-1} related to C=C stretching vibrations confirmed attendance of lignin and aromatic carbon.[45] The IR band peak at 1169 cm^{-1} is related to C–O–C symmetric stretching in ester groups of cellulose and hemicellulose.[46] Further, a peak below 900 (770–750) cm^{-1} related to C–O–C stretching vibrations pointed to the existence of aromatics and their derivatives in char.[46] Overall, the FTIR analysis of char confirmed that JCTB is a more functional group than NRPET and has a higher peak depth. However, loading of NRPET with JCT reduced the intensity and functional group of the char.

3.8 Raman analysis of char

The Raman spectra of JCTB, NRPETB, and JCTB + NRPETB blends (30, 50, and 80 wt%) in Fig. 8 highlight the graphitic nature of the char. Two prominent peaks, the D peak (~1350 cm^{-1}) and the G peak (~1573 cm^{-1}), were identified in each char.[31] The G peak is linked to graphite crystallinity, while the D peak indicates turbostratic or disordered carbon within the char structure.[32] The I_D/I_G intensity ratio is an indicator of structural disorder; a lower I_D/I_G suggests higher graphitic purity.[32] The 4-peak fitting analysis, as seen in Table 3, shows that NRPETB has a low I_D/I_G ratio, suggesting it has the most graphitic carbon, while JCTB, with a higher ratio, has less graphitic content.[32] This trend is consistent with the char's elemental composition in Table 2. Notably, blending NRPET with JCT at 30%, 50%, and 80% reduces the I_D/I_G values, indicating an increase in graphitic carbon content due to the rise in disordered carbon from microscopic structural degradation.[31] This demonstrates that combining plastic with biomass raises the graphitic carbon content in char.

3.9 SEM analysis of char

The surface morphology of the char was determined using an SEM analyser and is listed in Fig. 9a–e. The surface morphology of JCTB was found to be rough, porous, and irregular (Fig. 9a). In contrast, NRPETB was found to be very smooth and harder than JCTB (Fig. 9b). Char obtained from biomass pyrolysis tends to have rough and irregular surfaces because biomass is composed of complex organic polymers like cellulose, hemicellulose, and lignin. These components decompose unevenly at different temperatures, creating a porous, irregular structure. Additionally, biomass often contains minerals and inorganic compounds that can further contribute to surface roughness and intricate pore networks.[47] In contrast, plastics are synthetic polymers with more homogeneous molecular structures, lacking the natural fibrous matrix and mineral content found in biomass. This results in a more uniform thermal decomposition process during pyrolysis, leading to smoother, less porous char surfaces with more regular morphology.[47] Further, it was noticed that bleeding of NRPET at 30, 50 and 80 wt% with JCT increased the smoothness and hardness of the char surface morphology due to the addition of plastics. The blending of NRPET at 30 wt% with JCT increased the surface structure and hardness slightly (Fig. 9c), whereas adding NRPET at 50 wt% with JCT increased the surface structure and hardness significantly (Fig. 9d). Finally, adding NRPET at 80 wt% with JCT substyle increased the surface structure and hardness (Fig. 9e). Among 30, 50, and 80 wt% loading of NRPET on JCT, the surface structure and hardness of the char were increased to be in the following order: 33, 50 and 80 wt%. Overall, the addition of plastics with biomass increased the carbon content, hardness and surface morphology of the chars.

4 Conclusions

The co-pyrolysis of low-value wood sawdust and non-recyclable plastics offers an effective method for converting waste materials into valuable char. The study found that increasing plastic content in the blend led to a decrease in char yield, with reductions of up to 12.47%. However, the presence of plastics significantly enhanced the physicochemical properties of the char, including carbon content, heating value, and bulk density, while reducing the oxygen content and surface area. This suggests that blending plastics with biomass not only improves the char's quality but also increases its potential for use in energy storage and other industrial applications. FTIR, Raman, and SEM analyses confirmed that the blending process altered the functional groups and the structural characteristics of the char, making it more suitable for practical use. These findings underscore the potential of co-pyrolysis as a sustainable solution for plastic waste disposal and biomass valorisation.

Data availability

The datasets generated during and/or analysed during the current study are available from the corresponding author upon reasonable request.

Author contributions

Ranjeet Kumar Mishra: data collection and interpretation; conceptualisation, data curation, investigation, experimentation, visualisation, writing-original draft, review and editing.

Conflicts of interest

The authors have no relevant financial or non-financial interests to disclose.

Acknowledgements

The author would like to thank Biomass, Bioenergy and Bioproduct Lab (BBBL), Department of Chemical Engineering, Manipal Institute of Technology Manipal, Karnataka, for providing all the supporting facilities.

References

1 R. Thahir, M. Irwan, A. Alwathan and R. Ramli, *Results Eng.*, 2021, **11**, 100231.
2 H. L. Chen, T. K. Nath, S. Chong, V. Foo, C. Gibbins and A. M. Lechner, *SN Appl. Sci.*, 2021, **3**, 1–15.

3 C. J. Rhodes, *Sci. Prog.*, 2019, **102**, 218–248.
4 C. C. Seah, C. H. Tan, N. Arifin, R. Hafriz, A. Salmiaton, S. Nomanbhay and A. Shamsuddin, *Results Eng.*, 2023, **17**, 100989.
5 A. Priya, G. Anusha, S. Thanigaivel, A. Karthick, V. Mohanavel, P. Velmurugan, B. Balasubramanian, M. Ravichandran, H. Kamyab and I. M. Kirpichnikova, *Bioprocess Biosyst. Eng.*, 2023, **46**, 309–321.
6 M. Wu, Z. Wang, G. Chen, M. Zhang, T. Sun, Q. Wang, H. Zhu, S. Guo, Y. Chen and Y. Zhu, *J. Energy Inst.*, 2023, **111**, 101392.
7 R. Hossain, M. T. Islam, A. Ghose and V. Sahajwalla, *J. Cleaner Prod.*, 2022, **368**, 133127.
8 M. Kardung, K. Cingiz, O. Costenoble, R. Delahaye, W. Heijman, M. Lovrić, M. van Leeuwen, R. M'barek, H. van Meijl and S. Piotrowski, *Sustainability*, 2021, **13**, 413.
9 N. Tripathi, C. D. Hills, R. S. Singh and C. J. Atkinson, *npj Clim. Atmos. Sci.*, 2019, **2**, 35.
10 N. Dahmen, I. Lewandowski, S. Zibek and A. Weidtmann, *GCB Bioenergy*, 2019, **11**, 107–117.
11 T. Thiounn and R. C. Smith, *J. Polym. Sci.*, 2020, **58**, 1347–1364.
12 R. K. Mishra, S. Vijay, S. Soni, B. S. Dhanraj, P. Kumar and K. Mohanty, *J. Energy Inst.*, 2024, **114**, 101651.
13 F. Amalina, A. S. Abd Razak, S. Krishnan, A. Zularisam and M. Nasrullah, *Cleaner Mater.*, 2022, **3**, 100045.
14 A. G. Daful and M. R. Chandraratne, Biochar production from biomass waste-derived material, in *Encyclopedia of Renewable and Sustainable Materials*, 2020, pp. 370–378.
15 R. K. Mishra and K. Mohanty, *Sci. Total Environ.*, 2023, **904**, 167171.
16 B. B. Uzoejinwa, X. He, S. Wang, A. E.-F. Abomohra, Y. Hu and Q. Wang, *Energy Convers. Manage.*, 2018, **163**, 468–492.
17 S.-Y. Oh and Y.-D. Seo, *Bioresour. Technol.*, 2016, **218**, 77–83.
18 M. Sajdak, *J. Anal. Appl. Pyrolysis*, 2017, **124**, 415–425.
19 B. Fekhar, *et al.*, Co-Pyrolysis of Biomass and Plastic Wastes: Investigation of Apparent Kinetic Parameters and Stability of Pyrolysis Oils, in *IOP Conference Series: Earth and Environmental Science*, IOP Publishing, 2018, vol. 154.
20 E. Önal, B. B. Uzun and A. E. Pütün, *Energy Convers. Manage.*, 2014, **78**, 704–710.
21 L. Chen, S. Wang, H. Meng, Z. Wu and J. Zhao, *Appl. Therm. Eng.*, 2017, **111**, 834–846.
22 M. Vaishnavi, P. M. Vasanth, S. Rajkumar, K. P. Gopinath and Y. Devarajan, *J. Anal. Appl. Pyrolysis*, 2023, **170**, 105907.
23 T. Sun, Z. Li, Z. Zhang, Z. Wang, S. Yang, Y. Yang, X. Wang, S. Liu, Q. Zhang and T. Lei, *Bioresour. Technol.*, 2020, **301**, 122739.
24 J. B. Sluiter, K. P. Michel, B. Addison, Y. Zeng, W. Michener, A. L. Paterson, F. A. Perras and E. J. Wolfrum, *Cellulose*, 2021, **28**, 1989–2002.
25 A. Sluiter, B. Hames, R. Ruiz, C. Scarlata, J. Sluiter, D. Templeton and D. Crocker, Determination of structural carbohydrates and lignin in biomass, *Technical Report NREL/TP-510-42618*, National Renewable Energy Laboratory, 2008.
26 R. K. Mishra and K. Mohanty, *Bioresour. Technol.*, 2018, **251**, 63–74.
27 A. K. Varma, L. S. Thakur, R. Shankar and P. Mondal, *Waste Manage.*, 2019, **89**, 224–235.
28 R. K. Singh, B. Ruj, A. K. Sadhukhan and P. Gupta, *J. Energy Inst.*, 2020, **93**, 1020–1035.
29 T. Väisänen, K. Laitinen, L. Tomppo, J. Joutsensaari, O. Raatikainen, R. Lappalainen and P. Yli-Pirilä, *Indoor Built Environ.*, 2018, **27**, 194–204.
30 E. Watt, M. A. Abdelwahab, M. R. Snowdon, A. K. Mohanty, H. Khalil and M. Misra, *Sci. Rep.*, 2020, **10**, 10714.
31 R. K. Mishra, M. Misra and A. K. Mohanty, *ACS Omega*, 2022, **7**, 1612–1627.
32 K. Agweh, M. R. Snowdon, R. K. Mishra, G. Chen, S. Vivekanandhan, A. K. Mohanty and M. Misra, *Biomass Convers. Biorefin.*, 2024, **14**, 28619–28633.
33 R. Liu, G. Liu, B. Yousaf, Z. Niu and Q. Abbas, *Renewable Sustainable Energy Rev.*, 2022, **153**, 111761.
34 K. Polat and E. A. Bursalı, *J. Mater. Cycles Waste Manage.*, 2019, 1–7.
35 W. Cai, X. Wang, Z. Zhu, R. Kumar, P. N. Amaniampong, J. Zhao and Z.-T. Hu, *Fuel*, 2023, **353**, 129210.
36 A. A. Shagali, S. Hu, H. Li, H. Chi, H. Qing, J. Xu, L. Jiang, Y. Wang, S. Su and J. Xiang, *Fuel*, 2023, **331**, 125724.
37 T. A. Vo, Q. K. Tran, H. V. Ly, B. Kwon, H. T. Hwang, J. Kim and S.-S. Kim, *J. Anal. Appl. Pyrolysis*, 2022, **163**, 105464.
38 N. Y. Abu-Thabit, C. Pérez-Rivero, O. J. Uwaezuoke and N. C. Ngwuluka, *J. Chem. Technol. Biotechnol.*, 2022, **97**, 3217–3240.
39 G. F. M. Cupertino, Á. M. da Silva, A. K. S. Pereira, F. M. Delatorre, J. G. M. Ucella-Filho, E. C. de Souza, D. Profeti, L. P. R. Profeti, M. P. Oliveira and D. Saloni, *Fuel*, 2024, **362**, 130761.
40 I. Wani, A. Sharma, V. Kushvaha, P. Madhushri and L. Peng, *J. Hazard., Toxic Radioact. Waste*, 2020, **24**, 04020048.
41 Y. P. Rago, F.-X. Collard, J. F. Görgens, D. Surroop and R. Mohee, *Energy*, 2022, **239**, 121859.
42 C. Das, S. Tamrakar, A. Kiziltas and X. Xie, *Polymers*, 2021, **13**, 2663.
43 K. R. Vanapalli, J. Bhattacharya, B. Samal, S. Chandra, I. Medha and B. K. Dubey, *J. Cleaner Prod.*, 2021, **278**, 123968.
44 I. F. Titiladunayo, A. G. McDonald and O. P. Fapetu, *Waste Biomass Valorization*, 2012, **3**, 311–318.
45 R. Janu, V. Mrlik, D. Ribitsch, J. Hofman, P. Sedláček, L. Bielská and G. Soja, *Carbon Resour. Convers.*, 2021, **4**, 36–46.
46 A. Y. Elnour, A. A. Alghyamah, H. M. Shaikh, A. M. Poulose, S. M. Al-Zahrani, A. Anis and M. I. Al-Wabel, *Appl. Sci.*, 2019, **9**, 1149.
47 K. Crombie, O. Mašek, S. P. Sohi, P. Brownsort and A. Cross, *GCB Bioenergy*, 2013, **5**, 122–131.